


Article

Pedestrian Interaction with a Novel Urban Light Rail Vehicle: Implications for Multi-Modal Crash Compatibility Standards

Callum J. D. Bethell ^{1,*} , Shubham Sharma ¹, James Winnett ^{1,2} and Darren J. Hughes ¹

¹ WMG, University of Warwick, Coventry CV4 7AL, UK; shubham.sharma@warwick.ac.uk (S.S.); d.hughes@warwick.ac.uk (D.J.H.)

² Penmark Limited, The Mills Canal Street, Derby DE1 2RJ, UK

* Correspondence: callum.bethell@warwick.ac.uk; Tel.: +44-7913-187622

Abstract: This work investigates the risk to Vulnerable Road Users (VRUs) from a novel light rail vehicle using the pedestrian impact scenario outlined in CEN/TR 17420. At a 20 km/h impact speed, a maximum head impact criterion (HIC₁₅) value of 15.9 was obtained for a 50th-percentile anthropometric test device (ATD), with this value increasing to 120.2 at 30 km/h impact speed. Both results are within the CEN/TR 17420 prescribed limit of 1000. In both cases, the vehicle does not fully comply with CEN/TR 17420 recommendations due to insufficient lateral displacement of the ATD post-impact. A vehicle front-end design—which would be exempt from the CEN/TR 17420 impact testing—was designed and tested to the same framework. Despite being formally exempt from testing, the design also did not fully comply with CEN/TR 17420 lateral displacement requirements. Critical evaluation of the CEN/TR 17420 framework is presented, leading to recommendations about how updated frameworks should take a pragmatic approach in how they define VRUs, and the measurement criteria used for assessing VRU risk in collisions. Discussions are presented considering whether alternative frameworks, such as the Bus Safety Standard, should be applicable to assess the safety of the novel light rail vehicle.

Keywords: crash compatibility; vulnerable road user; light rail; head impact criterion; front-end design; pedestrian safety



Citation: Bethell, C.J.D.; Sharma, S.; Winnett, J.; Hughes, D.J. Pedestrian Interaction with a Novel Urban Light Rail Vehicle: Implications for Multi-Modal Crash Compatibility Standards. *Future Transp.* **2024**, *4*, 1177–1204. <https://doi.org/10.3390/futuretransp4040057>

Academic Editors: Andrew Morris and Jo Barnes

Received: 26 June 2024

Revised: 25 September 2024

Accepted: 8 October 2024

Published: 14 October 2024



Copyright: © 2024 by the authors. Licensee MDPI, Basel, Switzerland. This article is an open access article distributed under the terms and conditions of the Creative Commons Attribution (CC BY) license (<https://creativecommons.org/licenses/by/4.0/>).

1. Introduction

It is widely recognised that decarbonisation is required across all sectors to mitigate against the worst effects of climate change. In the United Kingdom (UK), the transportation sector accounted for 26% of all greenhouse gas emissions in 2021, and since 2016 has been the sector with the highest greenhouse gas emissions [1]. Decarbonisation of the transportation sector was addressed by the *Ten Point Plan for a Green Industrial Revolution* [2], Point 5 of which involved decarbonising public transportation, including pledges to invest in the infrastructure as well as 4000 zero-emission buses.

In order to improve the environmental impact of the transportation sector, a modal shift and behavioural change in commuters is required. Light rail is recognised as an important sector for growth for the modal shift of commuters away from cars into lower-emission forms of transport [3] since it offers an attractive and comfortable alternative to the car. Introduction of new light rail services and expansion of existing services saw passenger mileage by light rail increase by over 500% between 1984 and 2017 [4].

Coventry is one of the cities in the UK that is working on the introduction of a new light rail system. The Coventry Very Light Rail (CVLR) project has led to development of a novel form of urban, rail-based public transportation, expected to operate in the city of Coventry. Unlike conventional modern light rail systems, the CVLR vehicle is single-carriage, with an innovative bogie design enabling a 15-metre turning radius [5]. An onboard battery for the vehicle as well as fast charging at stops along the route, known as “opportunity

charging”, means that the vehicle produces zero tailpipe emissions and has no requirement for overhead charging equipment [5]. The CVLR network is intended to be an alternative to private transportation such as the car and is designed to be an attractive solution to commuters. CVLR vehicles are expected to share road infrastructure with other road users, including cars, buses, and Vulnerable Road Users (VRUs). VRUs are defined in the Intelligent Transport Systems directive as “non-motorised road users, such as pedestrians and cyclists, as well as motor-cyclists and persons with disabilities or reduced mobility and orientation” [6].

Design work for the demonstrator vehicle for the CVLR project (Figure 1) was completed by Transport Design International (TDI), an organisation based in Stratford-upon-Avon, United Kingdom. The vehicle has a capacity for 56 passengers (20 seated), a length of 11 m, and an unladen mass of approximately 11 tonnes [7]. These dimensions are more akin to single-deck buses than conventional light rail vehicles, with light rail vehicles typically being up to 50 m in length.



Figure 1. Coventry Very Light Rail (CVLR) demonstrator vehicle.

This article assesses the crash compatibility of the novel CVLR vehicle in interactions with pedestrians. Section 2 (Research Background) is a literature review, which discusses the case for vehicle-to-pedestrian collision studies in bus and light rail sectors, explores how head injuries are assessed by the Head Injury Criterion (HIC) framework, and discusses current recommendations in light rail safety in vehicle-to-pedestrian collisions. Section 3 explains how collision scenarios—which are based on the pedestrian impact scenarios specified by the technical report CEN/TR 17420—have been constructed in a virtual, Finite Element Analysis (FEA) environment, with the CVLR vehicle colliding with a model of a 50th-percentile adult male. The purpose of these experiments is to validate whether the novel geometries of the CVLR vehicle are compatible with pedestrians in collision scenarios.

Section 4 contains the results of the experiments conducted in this report. In Section 5, we discuss the outcomes of the conducted experiments, critically evaluate the CEN/TR 17420 framework, and describe recommendations for future research regarding the safety assessment of VRUs in collisions with light rail vehicles. Recommendations are made for areas where future research should be conducted to enable a framework to be representative of light rail interactions with a greater scope of VRUs, as well as to identify injury risk criteria applied in automotive safety that have not been applied in the CEN/TR 17420 guidelines for light rail vehicles.

2. Research Background

2.1. Vehicle-to-Pedestrian Interactions

As a “hop-on, hop-off” public transportation system operating on city streets, accident data from the bus and coach sector highlight the potential risk to pedestrians and other VRUs from services such as CVLR. In the United Kingdom, buses and coaches are involved in a disproportionately high number of pedestrian casualties on roads. Department for Transport (DfT) road traffic data show that buses and coaches were responsible for 0.6% of mileage covered on UK roads in 2021 [8]; however, between 2016 and 2021, buses and coaches were involved in 2.8% of road accidents that caused pedestrian casualty [9].

Statistical analysis of collisions between trams and pedestrians has also been conducted. In Prague, a city in which it is estimated that trams cover almost 38 million km of travelled distance per year [10], accident statistics for trams were collected. Between the years 2007 and 2020, a total of 1233 accidents between trams and pedestrians were reported, of which 56 resulted in fatalities [11].

Light rail interactions with VRUs pose particularly high risks compared to other types of interactions. A previous study analysed tram-to-pedestrian and automobile-to-pedestrian collisions and concluded that a light rail vehicle is 2.5 times more likely to fatally injure a pedestrian than a car at an impact speed of 50 km/h [12], with higher fatality rates at low speeds observed being attributed to run-over. Pedestrians are also more vulnerable than other road users to serious injury or fatality in collisions. A study in the US has highlighted how VRUs are disproportionately likely to die in collisions involving light rail vehicles. Whilst 19% of collisions involving light rail or streetcar vehicles in the US between 2011 and 2013 involved hitting a person, these collisions were responsible for over 80% of all fatalities from accidents involving light rail vehicles [13]. It is therefore crucial that factors affecting survival outcomes for pedestrians in collisions with trams, such as crash compatibility with pedestrians, are considered in the design of light rail vehicles and infrastructure.

In the bus and coach sector, several techniques have been identified as suitable for mitigating against pedestrian injuries in collisions, with many of these applicable to light rail vehicles. A study conducted on behalf of Transport for London (TfL) investigated design characteristics of buses that would reduce the risk to pedestrians, identifying three key features that could prevent pedestrian casualties [14]. The vertical rake angle is where the windshield and/or body at the front end of the bus is slanted inwards so that, in the event of a collision, the energy of an impact is dissipated over a longer period, reducing the forces on the VRU, causing the vehicle to hit the VRU gradually. Buses typically have a vertical rake angle of approximately 10°. Windscreen wiper motors may be mounted at the top of the windscreen on newer vehicles as opposed to at the base of the windscreen, reducing the likelihood that the head or body of the VRU would hit the motors, which are a hard and sharp structure. Additionally, lateral curvature of the front end of a vehicle enables a VRU to be deflected away from the path of a vehicle during a collision, preventing the VRU from being run-over by the vehicle [15].

Previous studies have investigated how changes to the front-end geometry of buses may prevent injury to pedestrians in frontal impact scenarios. Martin et al. assessed pedestrian injury likelihoods for three frontal profiles of buses: a previous-generation bus (which appears to be a Wrightbus Gemini 2), a current-generation bus (produced c. 2020) and a “parametric” bus model [16]. The parametric model is based on current-generation buses but with enhanced rake transition height, which is the height from the ground to the point at which the rake angle starts, as well as enhanced vertical and lateral rake angles. Results of the study showed that, at collision speeds of 30 mph (51 km/h), the likelihood of a serious-to-fatal head injury for a pedestrian reduced from 69% for a previous-generation bus to 44% for a current-generation bus, and enhancements to the geometry of current-generation buses have the potential to reduce this risk to below 20%.

2.2. Head Injury Criterion (HIC)

Head Injury Criterion (HIC) is a numerical assessment of the injury risk to people involved in a collision, and originated as a tool in automotive and sports science sectors, with HIC values based on the acceleration response of the head [17]. Physical testing of HIC is typically achieved using an anthropometric test device (ATD), in which acceleration of the head is tracked over time using accelerometers. The HIC equation (Equation (1)) is used to quantify the severity of impact to the head from the acceleration–time data, with acceleration, $a(t)$, measured in standard acceleration due to gravity, g ($g = 9.81 \text{ m s}^{-2}$) [18]. Time values (t_1 and t_2) are measured in seconds.

$$HIC = \left\{ \left[\frac{1}{t_2 - t_1} \int_{t_1}^{t_2} a(t) dt \right]^{2.5} (t_2 - t_1) \right\}_{max} \tag{1}$$

HIC values are categorised by the time period for which acceleration is considered, with HIC_{15} denoting a time period for the acceleration being observed ($t_2 - t_1$) lasting 15 ms, and HIC_{36} denoting a time period ($t_2 - t_1$) of 36 ms. The power factor of 2.5 accounts for duration and the weighted value of acceleration in the time period between t_1 and t_2 [19].

HIC is a unit that quantifies the head injury risk by the magnitude of acceleration to the head in an impact. Increased speeds will induce higher forces, and therefore higher accelerations, on the head of a road user affected in a collision. The risks from such impacts can be reduced by designing vehicles that dissipate force more gradually over time, and therefore reduce peak acceleration of the head in an accident.

Whilst developed over 20 years ago, the use of HIC, specifically HIC_{15} , to assess injury risk, is still widely used in automotive safety assessments. The European New Car Assessment Programme (Euro NCAP) applied HIC_{15} in its updates to the protocol for adult occupant protection crash tests, which were implemented at the start of 2024 [20].

The natural log of the HIC_{15} value can be used to determine the probability of specific injury severities using the Abbreviated Injury Scale (AIS) categories. In 1993, Hertz identified a normal distribution relationship between the natural logarithm (Log_e) of the HIC_{15} value and injury severity [21]. Her research included determining the means and standard deviations for these normal distribution curves for the AIS2+ (moderate-to-fatal injury severity) to AIS4+ (severe-to-fatal injury severity) injury categories (Table 1).

Table 1. The mean and standard deviation values for the normal distribution of AIS categories, based on the natural logarithm of HIC_{15} values.

AIS Category	AIS Category Description	Mean	Standard Deviation
AIS2+	Moderate-to-fatal injury	6.96352	0.84664
AIS3+	Serious-to-fatal injury	7.45231	0.73998
AIS4+	Severe-to-fatal Injury	7.65605	0.60580

The American Association of Medical Assistants (AAMA) have published guidance for the use of specific injury criteria in the assessment of safety in accidents, such as road accidents. In 1998, the AAMA published guidance for the assessment of accidents using injury criteria [22]. The report stated a maximum threshold for HIC_{36} values in collision scenarios of 1000, for models that represent mid-sized males, mid-sized females, and 6-year-old children. Lower maximum thresholds are used for models representing children under the age of 6, accounting for increased injury risks to younger children when exposed to the same accident criteria.

In 1999, the AAMA published an updated version of the injury criteria guidance, which accounted for HIC_{15} assessments being used for assessing head injury risks in accidents [23]. Since HIC_{15} assesses a smaller maximum timeframe for head acceleration, and therefore identical acceleration–time data of the head in a collision would lead to a

lower value for HIC_{15} compared to HIC_{36} , the maximum allowable threshold is lower for HIC_{15} than for HIC_{36} . The AAMA recommended a maximum allowable HIC_{15} value of 700, for adults and children aged 6 or older, in assessments of crash safety.

2.3. Light Rail Best Practice—Pedestrian Safety

As an urban transportation system that uses rail-guided vehicles and would have a significant element of the system operating on highways, the CVLR vehicle is categorised as a tram, which is a specific type of light rail vehicle [24]. In 2020, the report CEN/TR 17420 was published, which proposes a framework for assessing crash compatibility of light rail vehicles with respect to pedestrians [25]. CEN/TR 17420 guidelines propose the use of ATD and rescue mannequins to represent pedestrians across the tests conducted. The CEN/TR 17420 framework recommends two collision scenarios for testing: Reference Collision Scenario A—pedestrian impact, where an ATD is simulated walking in front of a vehicle and is hit by the vehicle at a set speed; and Reference Collision Scenario B—run-over, with rescue mannequins representing the pedestrians that begin the test lying on the road.

This article only investigates the performance of the CVLR vehicle in the pedestrian impact test scenario. The recommended method for this test utilises ATDs that represent a 50th-percentile male and a 6-year-old child being impacted by the light rail vehicle at an impact velocity of 20 km/h (5.556 m s^{-1}) [25]. This article only completes pedestrian impact assessment with a 50th-percentile male ATD. The pedestrian is stationary at the point of impact to reflect the fact that a person walking has negligible momentum relative to a light rail vehicle at 20 km/h. Tests are conducted with the pedestrian in two different locations, defined by the tram width (TW), which is the distance from the centre point of the vehicle in the lateral axis to the edge of the vehicle. Tests are conducted with the ATD positioned at 15% TW and 50% TW (Figure 2). In this pedestrian impact test, the virtual ATD is used to record both the HIC and lateral deflection.

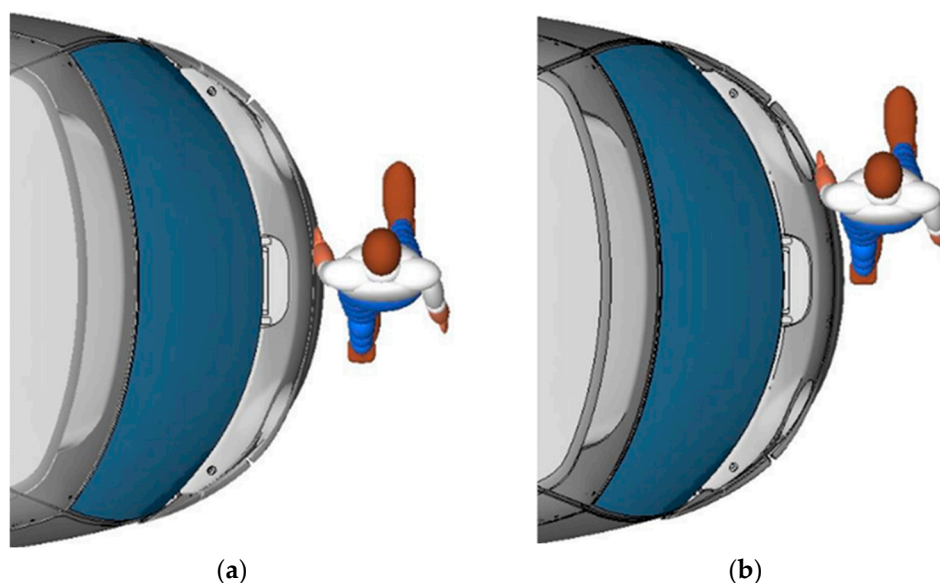


Figure 2. Pedestrian impact scenario, CEN/TR 17420. Diagrams of pedestrians located at (a) 15% TW; (b) 50% TW.

The CEN/TR 17420 guidelines use two criteria for assessing pedestrian safety in the scenario, as described previously. In order for the vehicle to pass the requirements of CEN/TR 17420, it must meet prescribed criteria for both the head impact and lateral deflection assessments. Firstly, a vehicle fails if the HIC_{15} value in any modelled collision scenario is equal to, or exceeding, a value of 1000. Secondly, for the 50% TW test, 15 ms after the conclusion of contact between the ATD and the vehicle, the ATD should be displaced laterally by a minimum of 800 mm, which demonstrates that the ATD is removed from the vehicle path and will therefore not be run-over following the initial collision. Therefore, the

CEN/TR 17420 pedestrian impact scenario addresses both the effects of the initial impact via the HIC_{15} criteria, and the lateral displacement to avoid secondary run-over following the primary impact.

Additionally, CEN/TR 17420 specifies front-end geometric features that would make a vehicle exempt from the requirements of the pedestrian impact test. In this case, the technical report prescribes that the vehicle can be assumed to be sufficiently safe in a vehicle-to-pedestrian collision (i.e., “the HIC_{15} value is assumed to stay below 1000”). A vehicle with these features is described herein to have “optimised front-end geometry”. Features of optimised front-end geometry are the curvature of the front end (α angles), which is based on the rake angle to the lateral axis at different points along the tram width, and the sloping of the front end (β angle), defined by the vertical rake angle at head height for a 50th-percentile male, which is defined as 1.75 m from the ground (Figure 3).

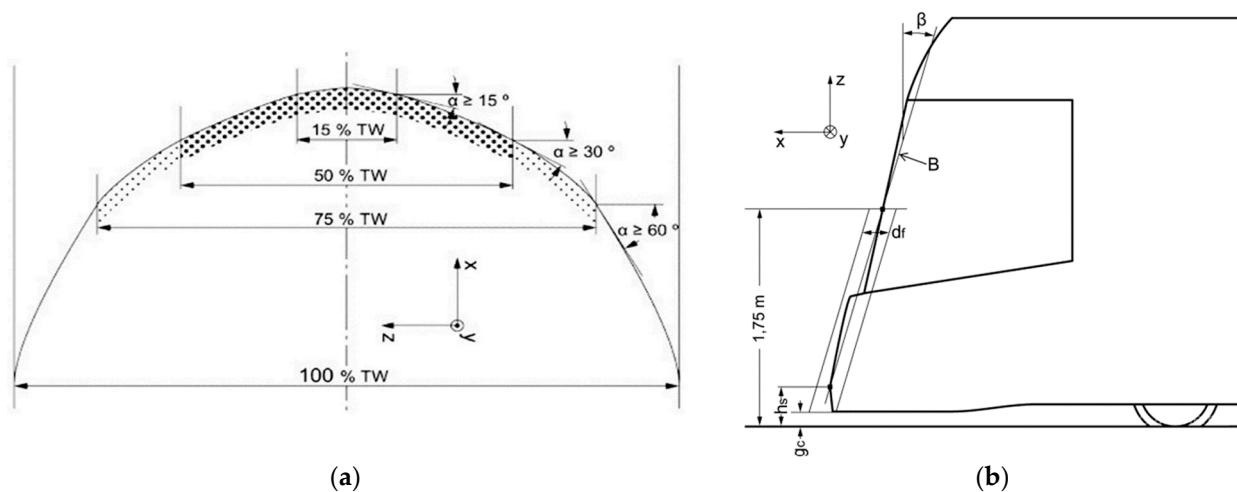


Figure 3. Pedestrian impact scenario, CEN/TR 17420. Diagrams demonstrating the required geometries to meet requirements for optimised front-end geometry for (a) frontal curvature; and (b) vertical rake profile.

Critical evaluations have been conducted on the developed CEN/TR 17420 frameworks in previous research. An article by Lackner et al. used accident data to identify aspects, such as collision speed, which should be prioritised in modelling tram-to-pedestrian collisions [26]. It was recognised that head injuries are the most prominent type of injury in tram-to-pedestrian collisions, justifying the use of HIC assessments in CEN/TR 17420. However, the article recommended that, in order to best capture conditions of accidents causing minor and severe pedestrian casualties, the impact speed in modelled collisions for impact testing should be increased to 30 km/h, from the 20 km/h set out in the CEN/TR 17420 framework.

Lackner also conducted research into the suitability of the CEN/TR 17420 definitions of “optimised front-end geometry” [27]. Their research compared HIC_{15} values for collisions between light rail vehicles and three different Human Body Models (HBMs), representing a 6-year-old child, a 50th-percentile male, and a 50th-percentile female at an impact speed of 20 km/h across various points of the width of a vehicle. Four vehicle shapes were assessed: a vehicle conforming to optimised front-end geometry; a vehicle conforming to the α angles only; a vehicle conforming to the β angle only; and a vehicle conforming to neither α nor β angles. For all three HBMs tested, the HIC_{15} values were lower for the vehicle with optimised front-end geometry, indicating lower risks of head injury to pedestrians for a vehicle with optimised front-end geometry. For all experiments of the vehicle front ends, the HIC_{15} values never exceeded the CEN/TR 17420 pass/fail threshold of 1000, and for all tests of the vehicle with optimised front-end geometry, the AAMA-recommended upper threshold for HIC_{15} values, 700 [23], was not exceeded.

3. Materials and Methods

3.1. Testing Overview

This work considers the pedestrian impact scenario outlined in CEN/TR 17420 for a 50th-percentile male. Experiments conducted for this study are split into three sections, each representing a specific scenario. Results from the data across all three experiments enable an assessment of the degree of vehicle safety to be completed as well as a critical evaluation of the suitability of CEN/TR 17420 for light rail vehicle safety. In all experiments the relevant criteria for HIC₁₅ and lateral deflection are assessed.

- Experiment A: A CVLR vehicle colliding with a pedestrian, impact speed = 20 km/h. Experiment A tests the existing CVLR vehicle to the existing recommendations made in CEN/TR 17420;
- Experiment B: A CVLR vehicle colliding with a pedestrian, impact speed = 30 km/h. Experiment B assesses the performance of the CVLR vehicle to the recommendations made by Lackner et al. [26], who argue that increasing the CEN/TR 17420 impact speed to 30 km/h better reflects accident scenarios, which cause more serious injury types;
- Experiment C: A light rail vehicle with “optimised front-end geometry” colliding with a pedestrian, impact speed = 20 km/h. Experiment C critically evaluates the validity of allowing exemptions from pedestrian crash compatibility testing for vehicles with optimised front-end geometries, which was proposed by CEN/TR 17420.

The experiments were conducted in a virtual environment, using the Finite Element Analysis software by Ansys, LS-DYNA (Oasys suite, Birmingham, UK, version 19.1). For all simulations, a version of the Hybrid-III (H-III), 50th-percentile male ATD was used (Figure 4) [28]. An ATD is a type of HBM that is designed specifically for crash testing and measuring injury severity in accident scenarios. The H-III ATD is widely used for crash testing across the transportation sector. The H-III dummy has articulation of joints, meaning that the ATD can be positioned in such a way to simulate a pedestrian walking; additionally, the dummy has features sensors that can measure the acceleration and deflection over time of particular parts of the body, such as the head and ribs.



Figure 4. Hybrid-III (H-III) anthropometric test dummy.

The size and gender of the HBM being used for testing have an impact on the results seen within testing since different HBMs and ATDs representing different people will have different geometries and therefore interact with the vehicle at different points. The guidelines for injury risk produced by the AAMA state the same HIC_{15} thresholds for models representing adults and children of age 6 or over [23]. However, research by Lackner assessed collisions between light rail vehicles that are compliant with CEN/TR 17420 definitions of optimised front-end geometry with HBMs representing a 50th-percentile adult male, a 50th-percentile adult female, and a 6-year-old child [27]. Higher HIC_{15} values were observed when a vehicle hit the HBM representing a 6-year-old child than when the same vehicle structure collided with an HBM representing a 50th-percentile male or 50th-percentile female adult, with lower HIC_{15} values observed for assessment against a 50th-percentile adult female. This shows that, for the same vehicle at the same speed, head injury risk is greater for a 6-year-old child in a collision with a light rail vehicle than it is for an adult.

3.2. CVLR Vehicle Model

The shell of the CVLR vehicle was simplified for virtual impact testing, with only components affecting the front-end stiffness modelled. Sections of the frontal cab structure were removed to leave the front profile only. The bumper, nose cone, wiper fairings, and windshield were the only other components modelled of the CVLR vehicle for this experiment, with components modelled as 2-dimensional shell-type finite elements (Belytschko–Tsay type with defined integration points and thickness). Modelling principles were derived from modelling structures in crash scenarios using non-linear explicit Finite Element Analysis (FEA). Final assembly involving the vehicle parts highlighted above were joined using massless, undeformed, node-to-node rigid connections available in LS-DYNA (Constrained_Spotweld).

In Experiment C, the optimised front-end structure was modelled via three components, with the windshield component made of glass held to a top section and a lower bumper part by spot-welds in LS-DYNA. As the CVLR vehicle is symmetrical in the XZ plane, the CEN/TR 17420 guidance states that the vehicle can be deemed safe with VRU impact tests being completed on one side of the front end. For simulations, the right-hand side of the vehicle was tested for the impact.

The CVLR vehicle body, including the bumpers and fairings, was assumed to be made of a carbon e-glass fibre composite. The material card for the composite material for these components was taken from previous research, which also involved modelling the CVLR vehicle in LS-DYNA [29]. An automotive glass was assumed to be the material for the windshield, with a material card formed using data from a previous study into pedestrian safety in automotive design [30]. In the Supplementary Materials, Table S1 shows the material card for the automotive glass used in this article, with Table S2 shows the material card for the carbon e-glass fibre composite used in this article.

When considering the position of the ATD relative to the tram width, the position of the ATD was defined by the centreline of the ATD. The ATD was set up in a standing position.

For Experiment C, an optimised front end was designed in CAD, in line with the definition of “optimised front-end geometry” within CEN/TR 17420 (Figure 5). The optimised front-end vehicle was designed to have the same width as the original CVLR vehicle. The body and windshield of the optimised front end have a vertical rake angle of 10° along the front of the vehicle. The curvature of the front end of the vehicle was designed so that the angles relative to the lateral plane are within the angle ranges specified in CEN/TR 17420.

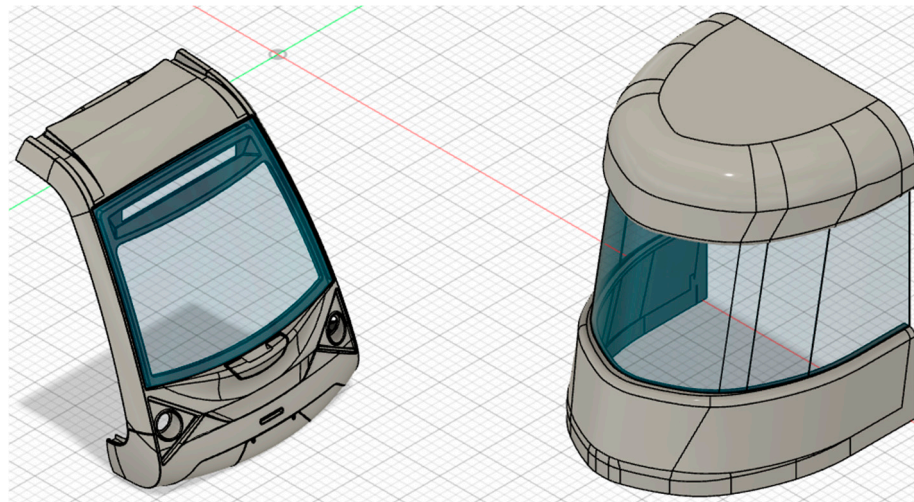


Figure 5. An image of the structure of the CVLR vehicle (**left**) and the concept structure that meets CEN/TR 17420 test immunity requirements (**right**).

In experiment C, the light rail vehicle front end with “optimised front-end geometry” is tested to the CEN/TR 17420 framework, with an ATD of a 50th-percentile male being hit by the front end at an impact speed of 20 km/h.

3.3. Assessment Design

Tests were conducted using the LS-DYNA software package, with double precision used for FEA calculations. Tests were generally performed over a period of 250 ms to fully capture the primary impact between the vehicle and the ATD, with timesteps of 0.1 ms used in the simulation. For some assessments, the simulation concluded prior to the 250 ms simulation time but tests were deemed valid if more than 15 ms had occurred between the end of contact between the vehicle and the ATD and the termination of the test. If contact had not terminated more than 15 ms prior to the end of the test, the assessment was repeated with the time increased, enabling the simulation to fully capture the contact period.

For the calculation of HIC_{15} values, data were captured for the acceleration magnitude of a single node in the head of the ATD. This position is where the accelerometer would be mounted in a physical H-III ATD. The acceleration magnitude was observed over time, with data filtered in post-processing using the SAE C1000 filter in Time History (T/His, Version 1.9) in the LS-DYNA suite. Filtered acceleration–time data were exported to a spreadsheet, where it was input into an author-developed tool that could obtain the area underneath the graph over a 15 ms period. This information was used to calculate the HIC_{15} value by identifying the maximum area underneath the graph and calculating the HIC_{15} value based on this area value.

The displacement of the ATD was measured from the average velocity in the lateral direction for the part named “pelvic” within the pelvis of the Hybrid-III ATD, as the centre of mass of the ATD is within the volume of the pelvic part. This component was chosen for the measurement of displacement since the CEN/TR 17420 guidelines do not state a particular point on the ATD where displacement is measured from. The average lateral-axis velocity over time of the pelvic part was extracted, filtered with the SAE C1000 filter in T/His (Version 1.9), exported into a spreadsheet, and integrated over the period for which the lateral displacement was measured. Manual inspection of each millisecond of simulated time was completed to identify the time when the ATD was no longer in contact with the CVLR front end, and 15 ms was added onto this—to determine the time for which the velocity of the pelvic part must be integrated—in order to calculate the lateral displacement of the ATD from the collision.

3.4. Preliminary Assessment—CVLR Vehicle

Preliminary assessments of the shape of the CVLR vehicle were conducted in order to assess whether the existing CVLR vehicle would comply with the definition of “optimised front-end geometry” specified in CEN/TR 17420. This inspection was conducted using the Computer Aided Design (CAD) model of the CVLR vehicle, with sketch lines used to draw the tangent angles to the frontal profile of the vehicle as well as lines in the lateral and vertical directions for measuring α and β lines, respectively. The measure tool on the design software was used to measure the rake angles by determining the angle between the relevant axis and the line tangential to the shape of the vehicle.

The CVLR vehicle does not achieve the required lateral rake angles (α angles) at any of the measured points across the tram width (Table 2). This is because the CVLR vehicle was designed with the philosophy of maximising passenger occupancy within a single-carriage vehicle. However, the vertical rake angle (β angle) exceeds the minimum 10° required for optimised front-end geometry, with an angle of approximately 30° seen. Therefore, were CEN/TR 17420 codified as a legislated standard, the CVLR vehicle would need to complete the pedestrian impact test.

Table 2. Minimum lateral and vertical rake angles for optimised front-end geometry (CEN/TR 17420) compared to CVLR angles at the same point.

Geometric Feature	Relative Position	Minimum Angle ($^\circ$)	CVLR Angle ($^\circ$)
Lateral rake angle (α)	15% TW	15	3.4
	50% TW	30	11.1
	75% TW	60	14.3
Vertical rake angle (β)	1.75 m Height	10	30.1

Having determined that the CVLR vehicle front-end geometry is not exempt from the CEN/TR 17420 framework, it was deemed necessary to conduct testing of the CVLR vehicle colliding with an ATD representing a pedestrian in order to assess whether the vehicle complies with CEN/TR 17420 recommendations.

4. Results

In summary, following the CEN/TR 17420 procedures for each experiment, HIC_{15} values were determined for the ATD in the 15% and 50% of the tram width (TW). An HIC_{15} value of less than 1000 is deemed a pass. Additionally, the lateral displacement of the ATD was measured for the 50% tram width impact. Furthermore, according to CEN/TR 17420 for the determination of the lateral displacement, the simulation was stopped 15 ms after the end of contact between the ATD and the tram. A lateral displacement of at least 800 mm is deemed to be a pass.

4.1. Experiment A (CVLR Vehicle, 20 km/h)

A summary of the results from Experiment A is provided in Table 3. For the 50% TW test conducted in Experiment A, contact between the ATD and vehicle had concluded after 66 ms of the simulated time, so displacement was measured after 81 ms from the initial contact. For the acceleration–time graphs of the head (Figures 6 and 7) the highlighted section depicts the region where HIC values are obtained from, where the area underneath the graph for a 15 ms period is at its maximum value. Figure 8 shows the lateral displacement of the pelvic ATD component for the 50% TW test.

Table 3. A summary of the HIC₁₅ results—with the pedestrian stood at 15% TW and 50% TW positions, and the lateral displacement results for the pedestrian stood at 50% TW position—for Experiment A.

Test Criteria	Value	CEN/TR 17420 Conformity
15% TW—HIC ₁₅ [No Units]	15.9	Pass
50% TW—HIC ₁₅ [No Units]	9.5	Pass
50% TW—Lateral displacement [mm]	53.8	Fail

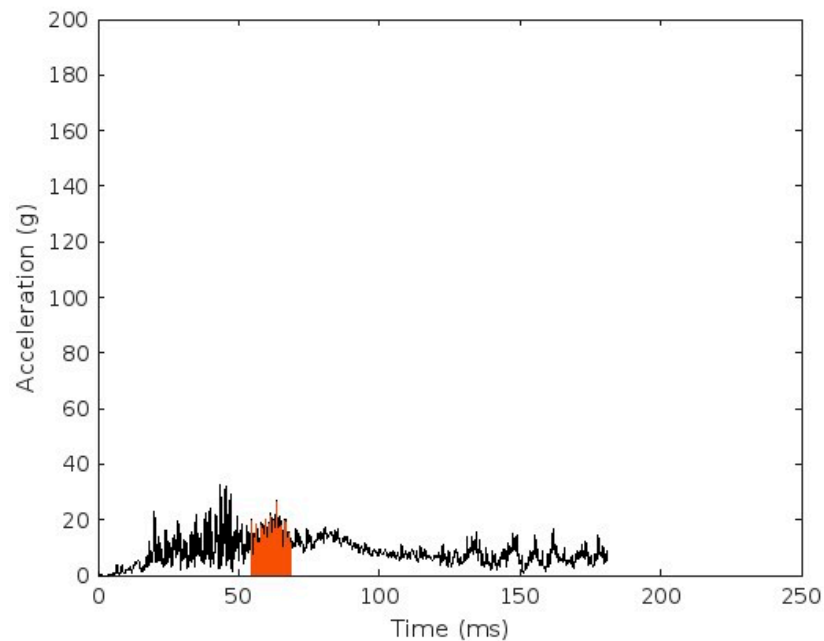


Figure 6. Acceleration–time graph of the head, Experiment A, 15% TW position (highlighted area beneath curve demonstrates the data employed to calculate the HIC₁₅ value).

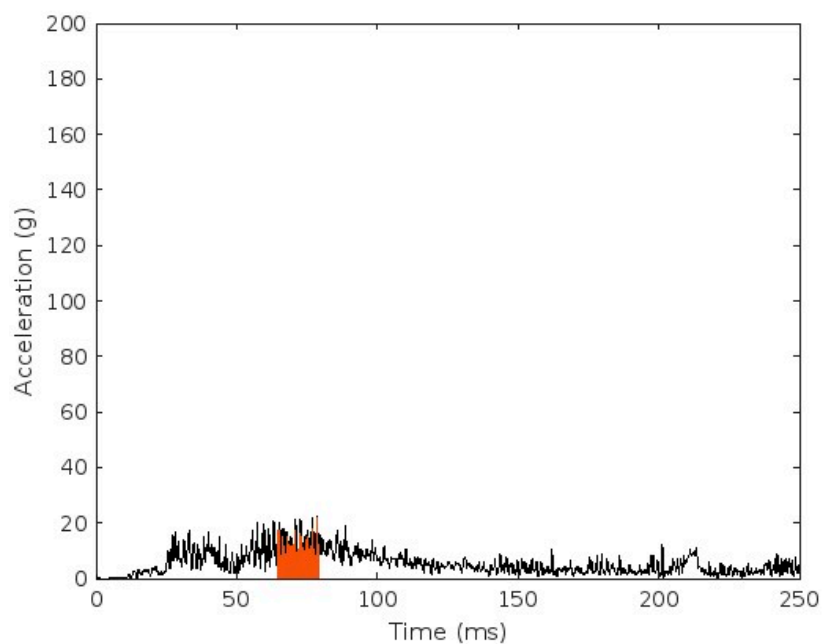


Figure 7. Acceleration–time graph of the head, Experiment A, 50% TW position (highlighted area beneath curve demonstrates the data employed to calculate the HIC₁₅ value).

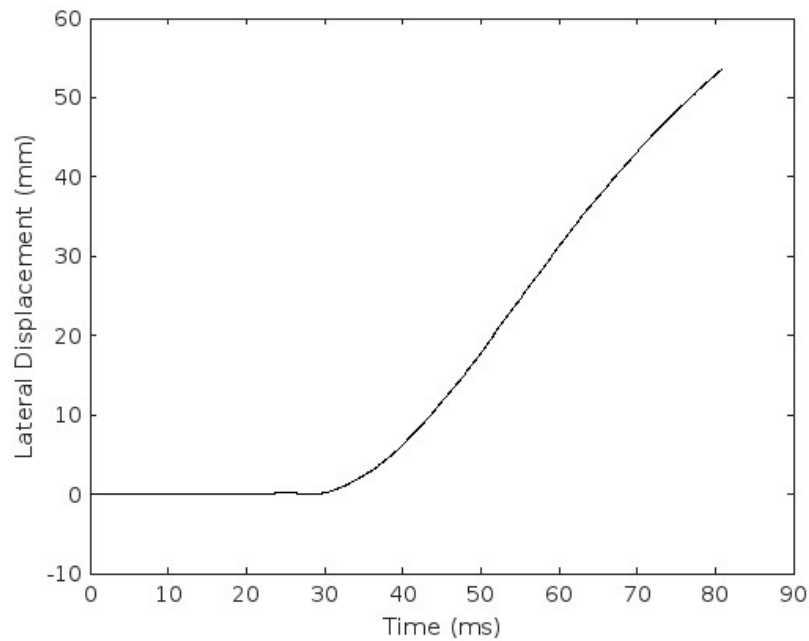


Figure 8. Displacement–time graph of pelvic part of the ATD, Experiment A, 50% TW position.

For Experiment A, for a collision speed of 20 km/h with the CVLR vehicle front end, HIC₁₅ values of 15.9 for the ATD in the 15% TW position and 9.5 for the ATD in the 50% TW position are seen. These are significantly below the 1000 maximum threshold for HIC₁₅ stated in the CEN/TR 17420 framework. With the ATD at the 50% TW position, a lateral displacement of 53.8 mm is seen, significantly short of the pass threshold for lateral displacement stated in the CEN/TR 17420 framework (800.0 mm).

4.2. Experiment B (CVLR Vehicle, 30 km/h)

A summary of the results from Experiment B is provided in Table 4. For the 50% TW test conducted in Experiment B, the contact between the ATD and vehicle had concluded after 90 ms of the simulated time, so displacement was measured after 105 ms from the initial contact. For the acceleration–time graphs of the head (Figures 9 and 10), the highlighted section depicts the region where HIC values are obtained from, where the area underneath the graph for a 15 ms period is at its maximum value. Figure 11 shows the lateral displacement of the pelvic ATD component for the 50% TW test.

Table 4. A summary of the HIC₁₅ results—with the pedestrian stood at 15% TW and 50% TW positions, and the lateral displacement results for the pedestrian stood at 50% TW position—for Experiment B.

Test Criteria	Value	CEN/TR 17420 Conformity
15% TW—HIC ₁₅ [No Units]	120.2	Pass
50% TW—HIC ₁₅ [No Units]	81.1	Pass
50% TW—Lateral displacement [mm]	111.4	Fail

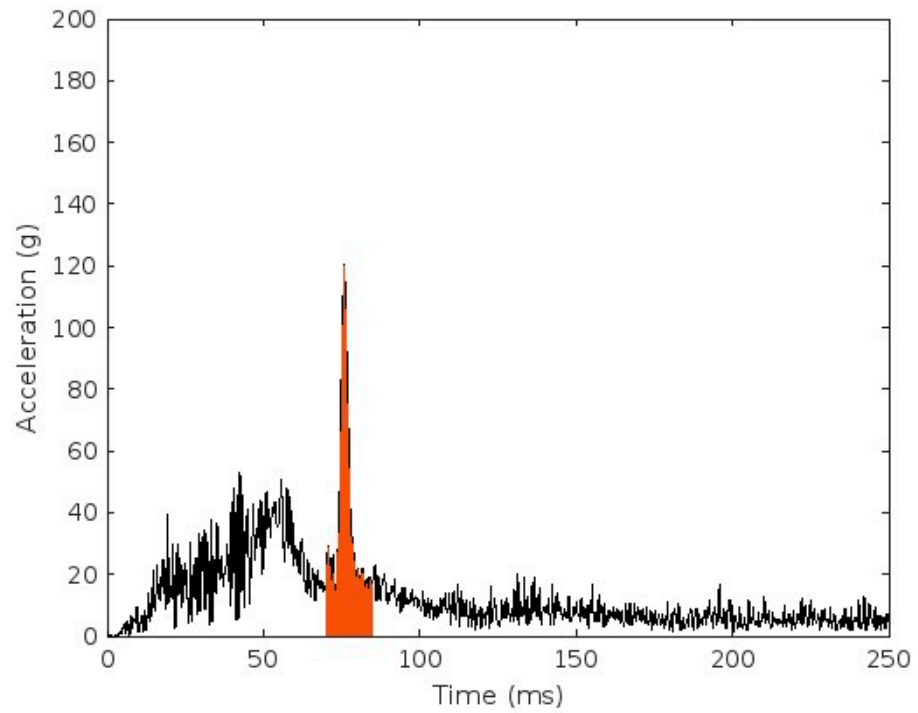


Figure 9. Acceleration–time graph of the head, Experiment B, 15% TW position (highlighted area beneath curve demonstrates the data employed to calculate the HIC₁₅ value).

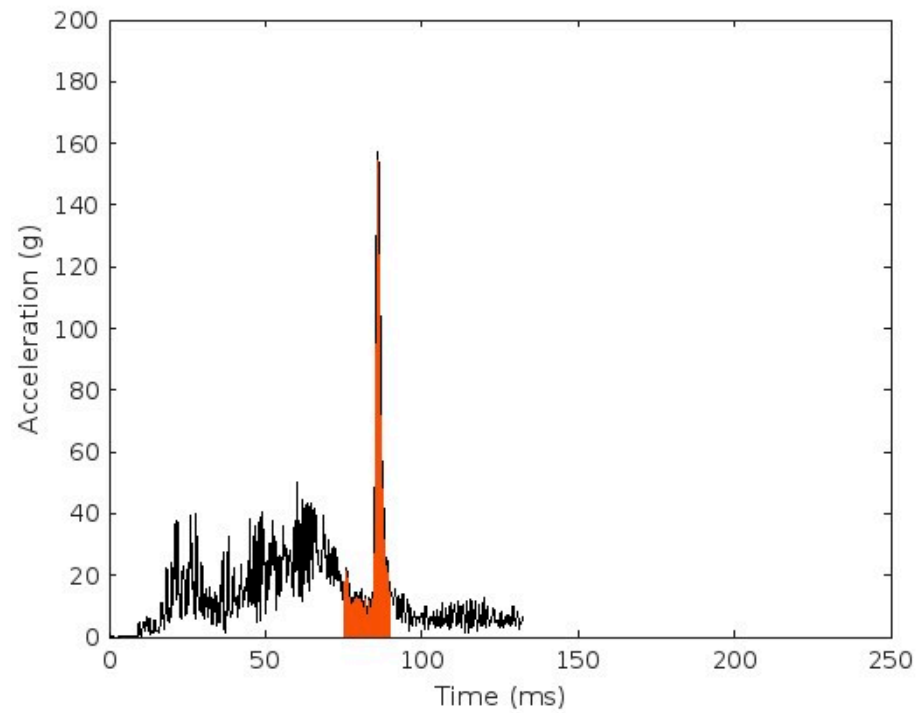


Figure 10. Acceleration–time graph of the head, Experiment B, 50% TW position (highlighted area beneath curve demonstrates the data employed to calculate the HIC₁₅ value).

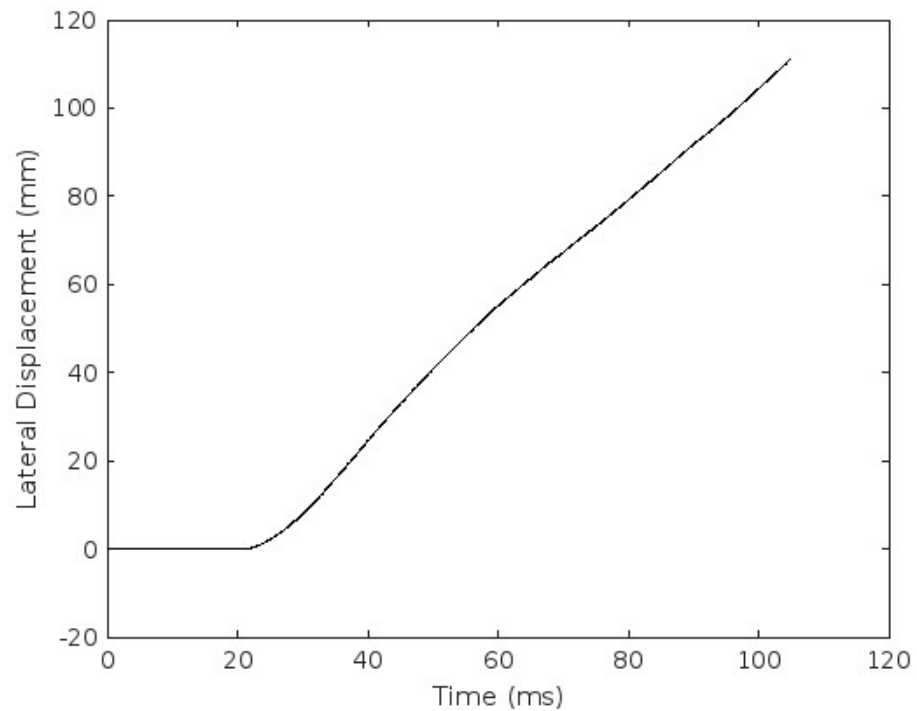


Figure 11. Displacement–time graph of the pelvic part of the ATD, Experiment B, 50% TW position.

For Experiment B, for a collision speed of 30 km/h for the CVLR vehicle front end, HIC₁₅ values of 120.2 for the ATD in the 15% TW position and 80.1 for the ATD in the 50% TW position are seen. These are significantly below the 1000 maximum threshold for HIC₁₅ stated in the CEN/TR 17420 framework. With the ATD at 50% TW position, a lateral displacement of 111.4 mm is seen, significantly short of the pass threshold for lateral displacement stated in the CEN/TR 17420 framework (800.0 mm).

4.3. Experiment C (Optimised Front-End Design, 20 km/h)

A summary of the results from Experiment C is provided in Table 5. For the 50% TW test conducted in Experiment C, the contact between the ATD and vehicle had concluded after 255 ms of the simulated time, so displacement was measured after 270 ms from the initial contact. This meant that, for this test, the total time simulated for the collision was increased to ensure that the full accident scenario was captured. For the acceleration–time graphs of the head (Figures 12 and 13) the highlighted section depicts the region where HIC values are obtained from, where the area underneath the graph for a 15 ms period is at its maximum value. Figure 14 shows the lateral displacement of the pelvic ATD component for the 50% TW test.

Table 5. A summary of the HIC₁₅ results—with the pedestrian stood at 15% TW and 50% TW positions, and the lateral displacement results for the pedestrian stood at 50% TW position—for Experiment C.

Test Criteria	Value	CEN/TR 17420 Conformity
15% TW—HIC ₁₅ [No Units]	9.3	Pass
50% TW—HIC ₁₅ [No Units]	63.7	Pass
50% TW—Lateral displacement [mm]	592.7	Fail

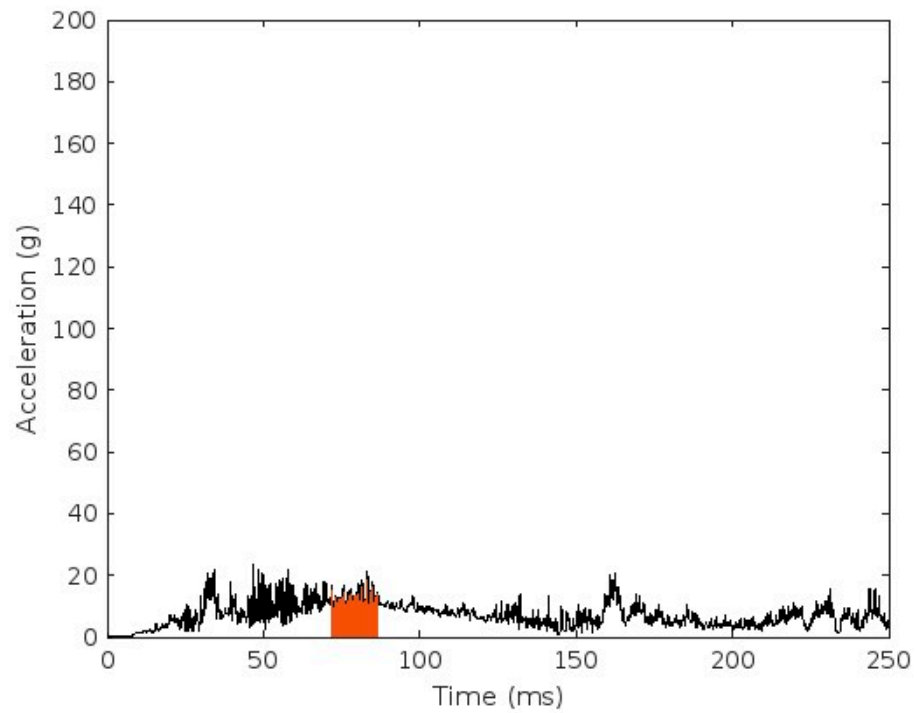


Figure 12. Acceleration–time graph of the head, Experiment C, 15% TW position (highlighted area beneath curve demonstrates the data employed to calculate the HIC₁₅ value).

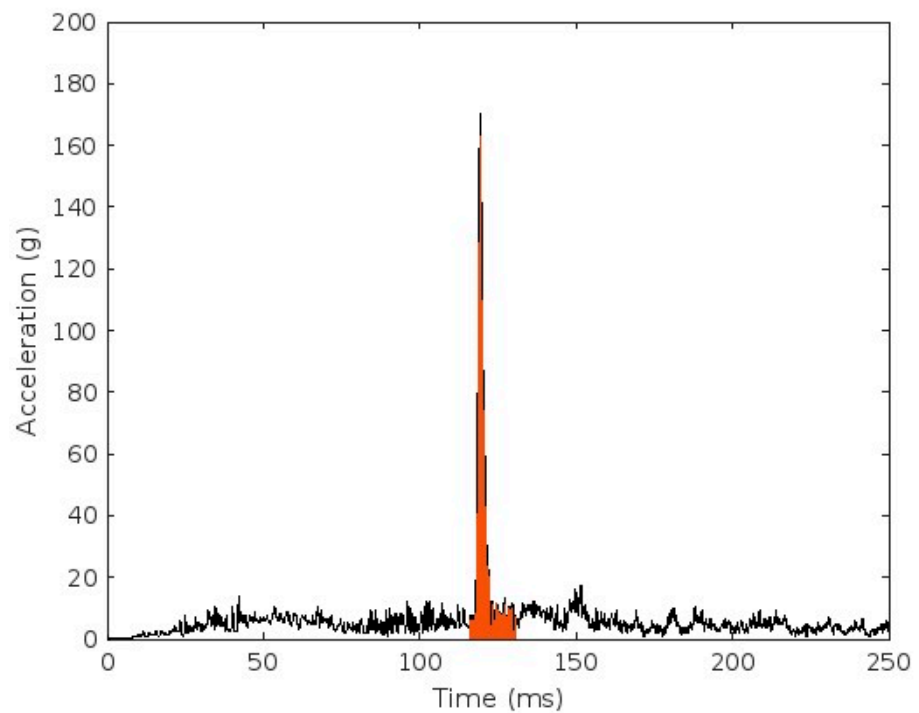


Figure 13. Acceleration–time graph of the head, Experiment C, 50% TW position (highlighted area beneath curve demonstrates the data employed to calculate the HIC₁₅ value).

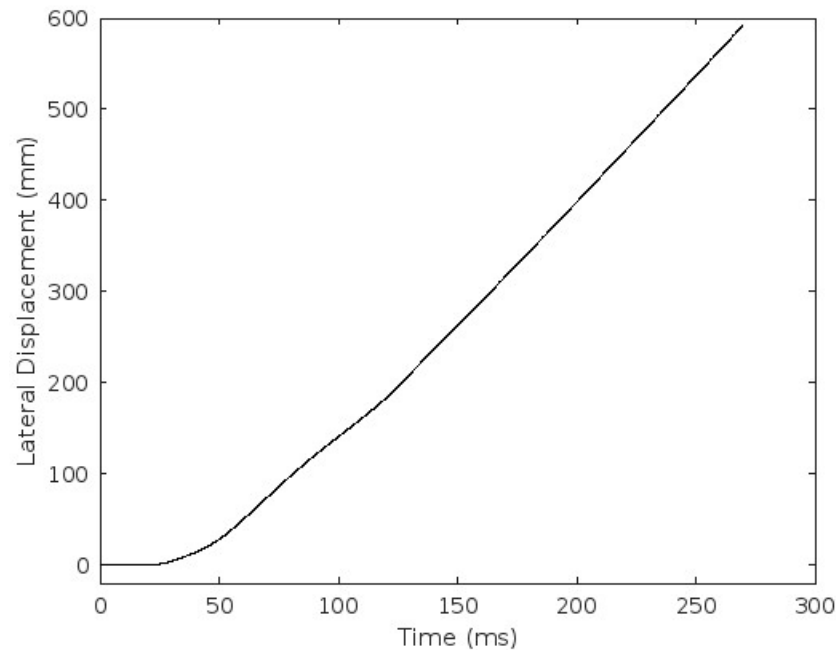


Figure 14. Displacement–time graph of pelvic part of the ATD, Experiment C, 50% TW position.

For Experiment C, for a collision speed of 20 km/h for a light rail vehicle with optimised front-end geometry, HIC_{15} values of 9.3 for the ATD in the 15% TW position and 63.7 for the ATD in the 50% TW position are seen. These are significantly below the 1000 maximum threshold for HIC_{15} stated in the CEN/TR 17420 framework. With the ATD at 50% TW position, a lateral displacement of 592.7 mm is seen, significantly short of the pass threshold for lateral displacement stated in the CEN/TR 17420 framework (800 mm).

5. Discussion

Captured footage for all of the collision scenarios and experiments conducted for this article have been provided, and can be found in Video S1 of the Supplementary Materials associated with this article.

5.1. Collision Kinematics

5.1.1. Experiment A (CVLR Vehicle, 20 km/h)

The HIC_{15} values seen in Experiment A are significantly lower than the maximum limit set out in the CEN/TR 17420 guidance of 1000. In the 15% TW position, the HIC_{15} value of 15.9 correlates to a likelihood of a head injury of moderate or worse (AIS2+) severity of under one-in-a-million. Head injury is therefore not expected if a collision between the CVLR vehicle and a pedestrian occurs at 20 km/h, with casualties in such collisions more likely to occur in other ways, as discussed later.

The lateral displacement over the assessed time period was only 53.8 mm, over 700 mm short of the 800 mm needed to comply with CEN/TR 17420. Failure to displace the ATD during the collision would leave the ATD vulnerable to being run-over. It is most likely that a combination of the limited frontal curvature on the CVLR vehicle and the relatively low impact speed is responsible for the low amounts of lateral displacement. A vehicle with a greater curvature of the front end would be expected to displace the ATD more laterally in an impact, pushing the ATD around the width of the vehicle and out of the vehicle path.

The collisions in Experiment A (at 15% TW and 50% TW) both have similar kinematics. Images have been presented of the 50% TW accident scenario (Figure 15) but the commentary on the ATD kinematics is applicable to both 15% and 50% TW collision scenarios.

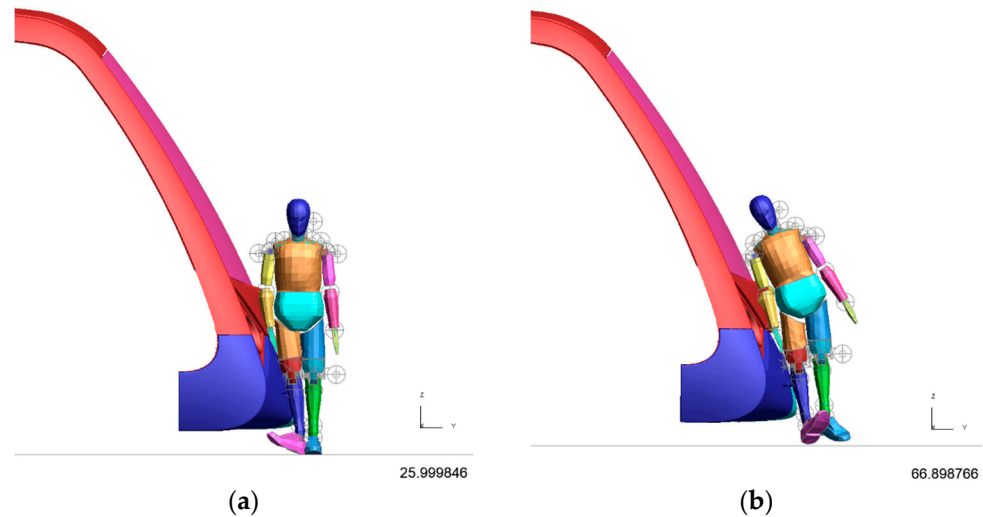


Figure 15. CVLR vehicle and H-III ATD at (a) initial contact and (b) end of contact, Experiment A, 50% TW position (vehicle travelling from left to right).

With the very front of the vehicle being at a height of approximately 200 mm off the ground, initial contact is made just above the ankle of the ATD, causing the first rise in head acceleration values. The ankle then twists, and as the vehicle progresses, contact occurs higher up on the ATD. Once the contact is at waist height on the ATD, the body of the ATD rotates onto the frame of the vehicle. Following this, the contact between the ATD and the ground is lost and, consequently, the ATD lifts upwards, leaning towards the vehicle’s front end. This causes another period of increased acceleration of the head.

The head of the ATD did not hit the windshield or the body of the vehicle in the impact at a speed of 20 km/h, and because of this, the HIC₁₅ values from the collision scenarios are low. Contact between the vehicle and ATD terminates as the ATD is pushed in front of the vehicle before contact with the head can occur.

5.1.2. Experiment B (CVLR Vehicle, 30 km/h)

When the speed of the CVLR vehicle at impact was raised to 30 km/h, the HIC₁₅ values were higher due to the increased collision speeds. However, the HIC₁₅ values in both tests of Experiment B remain significantly below the failure threshold of the 20 km/h test of 1000, meaning that the vehicle meets recommendations regarding head injury even when the speed is increased to 30 km/h. When head injury probability is assessed using the equations proposed by Hertz [21], at a collision speed of 30 km/h (18.6 mph), a maximum HIC₁₅ value of 120.2 (at 15% TW) means that a pedestrian has approximately a 0.02% chance of sustaining a serious (AIS3+) head injury, and just over 0.5% chance of sustaining a moderate (AIS2+) injury (Table 6).

Table 6. Injury probabilities for HIC₁₅ values using results from Experiment B, based on the Abbreviated Injury Scale (AIS).

HIC ₁₅ Value	AIS2+	AIS3+	AIS4+
120.2	0.51%	0.02%	0.00%
81.1	0.12%	0.0018%	[Minimal]

For both tests with the CVLR vehicle at an impact speed of 30 km/h, contact is made between the vehicle and the head of the ATD during the period where the HIC_{15} values are obtained. Despite this, HIC_{15} values of 120.2 and 81.1 are relatively low considering that the head of the ATD hits the windshield of the vehicle. This would suggest that the nature of the head contact is of relatively low force, and therefore presents a low degree of risk to the ATD.

The CVLR vehicle would fail to meet CEN/TR 17420 guidelines if the impact test was conducted at 30 km/h because the lateral displacement of the VRU is too small (111.4 mm) in the 50% TW test. As a result of this, the ATD is at risk of being struck again by the vehicle and run-over since it is not pushed out of the path of the vehicle.

The vehicle–ATD kinematics are similar for both 15% TW and 50% TW scenarios. Whilst images are shown from the 50% TW collision (Figure 16), commentary about the kinematics of the ATD is also applicable to the 15% TW collision scenario.

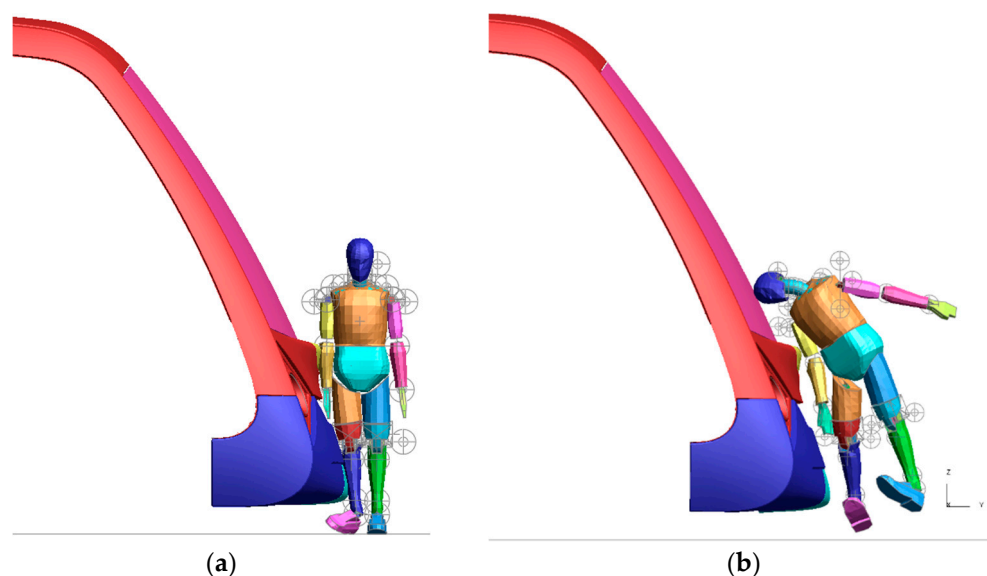


Figure 16. CVLR vehicle and H-III ATD at (a) initial contact, and (b) head contact, Experiment B, 50% TW position (vehicle travelling from left to right).

Contact in both collisions initiates just above the ankle, causing an initial spike in head acceleration for the ATD and the ankle to twist. The shape of the front end of the CVLR vehicle causes contact to be made higher up on the ATD gradually over the course of the impact. When the contact between the ATD and vehicle begins to occur around pelvic height, the legs are taken from under the ATD and the first major increase in acceleration values occurs. The torso of the ATD then begins to twist as the ATD falls onto the vehicle.

During the time when the ATD is falling whilst in contact, in both collisions, the head of the ATD hits the glass windshield of the CVLR vehicle. This causes a short peak in the acceleration values of the head, with this peak being the period where the HIC_{15} values are produced from the dataset. Whilst the ATD is still falling, in both collisions, it is pushed away from the front of the vehicle.

The lateral displacement of the ATD over the course of the collisions is greater than from Experiment A due to the higher impact speed, but in both cases, this lateral displacement is low compared to the vehicle width. If the simulation continued without deceleration of the vehicle, the ATD would engage with the lower section of the vehicle, which could cause run-over if additional deflectors are not present on the vehicle's front-end structure.

5.1.3. Experiment C (Optimised Front-End Design, 20 km/h)

The risk of head injury to a pedestrian in the primary impact is shown to be slightly greater for the vehicle with an optimised front-end design than it is for the CVLR vehicle.

The highest HIC_{15} value was seen with the ATD in the 50% TW position, with an HIC_{15} value of 63.7 being greater than the highest value of 15.9 seen in Experiment A (CVLR vehicle at 20 km/h). However, this value is still significantly below the threshold proposed in CEN/TR 17420 of 1000. Given that an HIC_{15} value of 63.7 correlates to a risk of moderate-to-fatal head injury (AIS2+) of under 0.05% [21], whilst the threshold HIC_{15} value of 1000 correlates to a 47% chance of AIS2+ severity head injury, this highlights how the risk to a VRU in interactions with a vehicle with curved front end is very low relative to the tolerable risks within the CEN/TR 17420 framework.

In the collision from the 50% TW position, a lateral displacement of the ATD of 592.74 mm was recorded. This would mean that the optimised front-end vehicle design would also fail to meet CEN/TR 17420 recommendations for 800 mm lateral deflection, despite being formally exempted from the test. It should be noted however that approximately 90 ms after the end of the primary collision, the lateral displacement of the pelvic component of the ATD did exceed 800 mm, demonstrating that the main body of the ATD would not have been run-over in the collision (Figure 17). By the point that the vehicle passes the ATD, the ATD is out of the path of the vehicle.

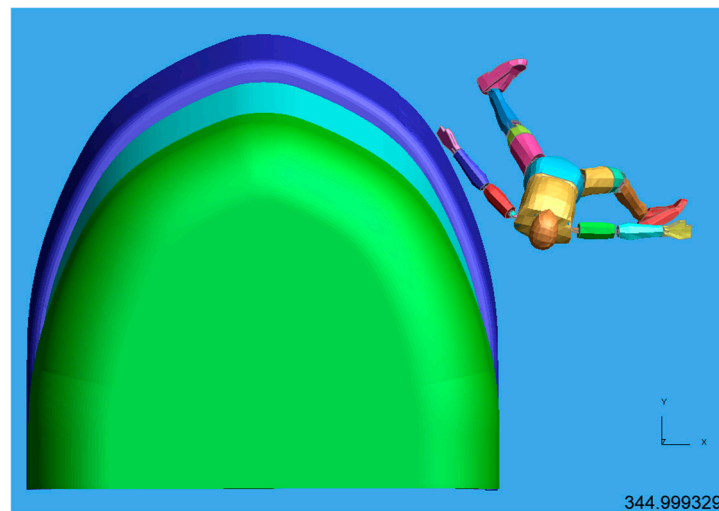


Figure 17. Position of the ATD relative to the vehicle, approximately 90 ms after the end of the primary collision (Experiment C, 50% TW) (vehicle travelling from bottom to top).

With the ATD standing in the 15% TW position, the reduced vertical rake angle of the optimised shell means that the collision affects the ATD close to the height of the centre of mass much earlier in the impact time compared to the CVLR vehicle (Figure 18). The body of the ATD twists and falls onto the body of the vehicle earlier in the collision scenario. As the ATD falls onto the vehicle, the torso rotates and the ATD begins to be displaced to the side of the vehicle during the impact time.

When the ATD is standing in the 50% TW position, as soon as they are hit by the vehicle, the ATD rotates so that their back gradually leans onto the vehicle profile (Figure 19). The ATD slides down the side of the vehicle, falling backwards onto the body of the vehicle in the collision. In the collision with the 50% TW position, the head of the ATD does hit the glass windshield of the vehicle, although the resultant acceleration from this contact is relatively low since there is a greater area of contact between the vehicle and ATD compared to previous collisions, enabling the force to be dissipated. This, however, accounts for the fact that the HIC_{15} value for the more central 15% TW impact is significantly lower than for the more offset 50% TW impact. Following this contact, the ATD is pushed forward and there is a break in the contact between the vehicle and ATD.

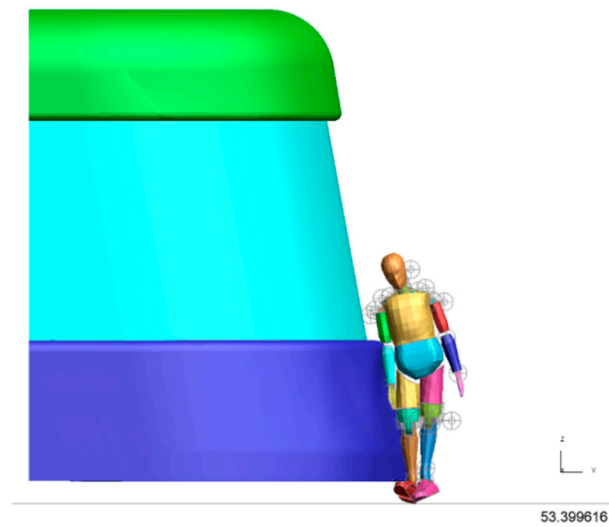


Figure 18. ATD in early contact with the vehicle, Experiment C, 15% TW (vehicle travelling from left to right).

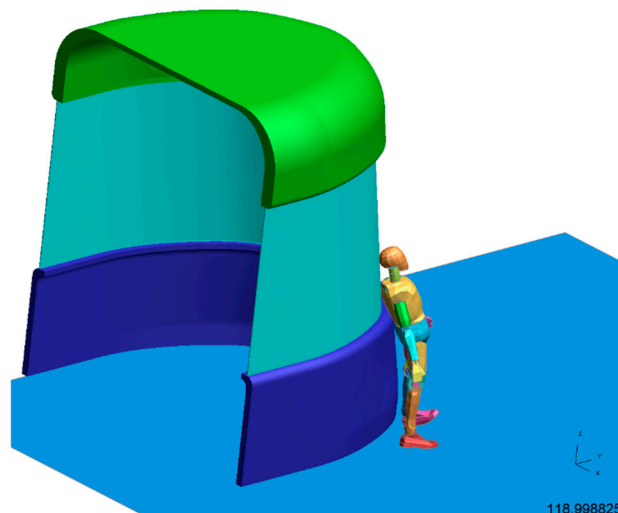


Figure 19. Contact between the head of the ATD and the vehicle, Experiment C, 50% TW.

5.2. Critical Evaluation—CEN/TR 17420

5.2.1. Incident Scenarios

The CEN/TR 17420 technical report considers two collision scenarios for light rail vehicles colliding with pedestrians: impact for a standing person, and run-over for a person lying down on the ground in front of the light rail vehicle. The impact scenario considers the initial impact phase, assuming that a collision between a light rail vehicle and a pedestrian would occur due to the pedestrian crossing in front of the vehicle. The run-over scenario assumes that the person is lying down on the road and investigates the suitability of the underrun protection of a vehicle. The purpose of the run-over scenario is to assess the risk of entrapment underneath the vehicle in the event of run-over.

Previous research has evaluated how suitable these tests are for capturing likely incident scenarios. Gaca and Franek analysed data from real-world collisions on Polish tram networks, finding that between 50% and 70% of all collisions involving a pedestrian and a light rail vehicle occurred in close proximity to a tram stop or at a pedestrian crossing [12]. The same research justified the run-over test, suggesting that run-over or entrapment underneath the light rail vehicle is a factor in many collisions at slower speeds that causes pedestrian fatality.

In this article, experiments were performed at both the CEN/TR 17420 recommended speed of 20 km/h and at a higher impact speed of 30 km/h. The HIC₁₅ values obtained at 30 km/h are higher than in the assessments conducted at 20 km/h, which is expected given the increase in collision speed. The kinematics of the vehicle travelling at higher speeds cause the head of the ATD to collide with the vehicle in the 30 km/h scenarios, whilst at 20 km/h, the ATD falls away from the vehicle without the head making contact.

Previous research has proposed increasing the impact speed in the CEN/TR 17420 recommendations to 30 km/h from the existing 20 km/h [26]. Our research supports this argument and shows an approximately 8-fold increase in HIC value at 30 km/h compared to 20 km/h. Such a change would enable the testing scenarios to be more representative of real-world interactions between pedestrians and light rail vehicles. Increasing the impact speed would also enable a better understanding of accidents of higher severity, as they would be captured more effectively by the testing procedure.

It is interesting to note that, whilst for tram-to-VRU collisions the CEN/TR 17420 report may capture the most relevant scenarios, most VRU casualties on the road are not pedestrians. For example, data from Transport for London (TfL) covered urban highway casualties between the start of 2019 and August 2023 [31]. During this time, 20,660 pedestrian casualties were reported, less than the amount for road users who travelled by pedal cycle (22,998 casualties) and powered 2-wheelers such as motorbikes (26,757 casualties). Therefore, whilst pedestrians are a specific risk group for light rail vehicles and buses in particular, they make up only 30% of VRUs who sustain injuries on roads in London.

5.2.2. Optimised Front-End Geometry

CEN/TR 17420 provides an exemption to virtual/physical testing for front-end designs meeting certain geometric conditions. As shown by Experiment C, a vehicle meeting the proposed definition of an optimised front-end design within CEN/TR 17420 would be sufficiently safe to prevent serious head injury to a pedestrian hit by a vehicle. This is evident by the low HIC₁₅ values obtained at the prescribed test speed of 20 km/h, which do not exceed 63.7.

In addition to the HIC₁₅ requirements, CEN/TR 17420 specifies that the pedestrian at the 15% TW position is displaced laterally at least 800 mm within 15 ms after contact between the pedestrian and vehicle terminates. The results here show that for the optimised front-end design, this condition is not met. Despite this, the simulation results showed that a vehicle with the optimised front-end design would eventually cause the pedestrian to be deflected out of the path of the vehicle at an impact speed of 20 km/h. This suggests that vehicles that do not have optimised front-end geometry, as stated by the technical report, likely face higher performance requirements than vehicles with optimised front-end geometry.

There are questions over the feasibility of a vehicle being able to laterally displace the ATD by the minimum 800 mm within 15 ms of contact termination at an impact speed of 20 km/h, regardless of the geometry of the vehicle. For a typical light rail vehicle with a width of 2650 mm, the mean lateral velocity of the ATD in the 15 ms after contact is broken would need to be at least 33 km/h (9.167 m s^{-1}) to achieve 800 mm displacement within 15 ms. This indicates that the lateral displacement pass/fail criteria stated for the pedestrian impact scenario in CEN/TR 17420 will, as a consequence, encourage the design of light rail vehicles only with an optimised front-end geometry since it is highly unlikely that a vehicle that does not have this geometry could achieve this minimum displacement in the time. Notably, even if a vehicle could achieve this, the lateral forces acting from the vehicle onto the ATD would increase the risks to the ATD of injury from secondary impact with the road.

Previous research shows that a vehicle with optimised front-end geometry should be safer for pedestrians than a vehicle that deviates from the characteristic α and β angles of optimised front-end design [27]. Lackner conducted research showing that when the ATD of a 6-year-old child replaced the ATD of a 50th-percentile male, the enhanced safety

of the front end—which conformed to the minimum β angle—was even more pronounced than with the 50th-percentile male ATD [27]. Vehicles that did not conform to both the α and β angles required for optimised front-end geometry performed significantly worse in the head impact assessments across both pedestrian locations along the front of the vehicle’s shell.

5.2.3. Criteria Assessed for Vehicle Safety

CEN/TR 17420 states that, for the pedestrian impact scenario, the failure threshold for HIC₁₅ values should be 1000 [25]. Previous recommendations made by the AAMA proposed that an HIC value of 1000 was the recommended maximum “acceptable” value for using HIC₃₆ to assess safety [22]. However, in 1999, the AAMA produced further guidance, proposing a maximum acceptable HIC₁₅ value of 700 for adults and children aged 6 years old or over [23]. Therefore, for the CEN/TR 17420 framework, a vehicle would be able to meet the recommendations for head injury risk, despite being deemed unsafe according to the AAMA guidelines for injury risk criteria. This is because the failure threshold for HIC₁₅ of CEN/TR 17420 guidelines, of 1000, is incompatible with the AAMA guidance for the HIC₁₅ fail threshold of 700.

If the probability equations modelled by Hertz [21] are used to assess injury risk based on the HIC₁₅ values, the likelihood of injury is significantly greater at HIC₁₅ values of 1000 compared to 700. Contact to the head at an HIC₁₅ value of 1000 as opposed to 700 leaves an individual over 50% more likely to experience a moderate-severity injury, over twice as likely to experience a serious injury, or over three times as likely to experience a severe injury (Table 7).

Table 7. Comparison of injury probabilities for HIC₁₅ values of 700 and 1000, based on the Abbreviated Injury Scale (AIS).

HIC ₁₅ Value	AIS2+	AIS3+	AIS4+
700	31.31%	11.16%	3.41%
1000	47.37%	23.09%	10.84%

The CEN/TR 17420 framework also does not account for the “3 ms” metric that is applied in various vehicle safety standards and recommendations, including the European New Car Assessment Programme (Euro NCAP) for automotive safety [20]. This criterion classifies that a vehicle fails a crash test if a continuous acceleration exceeding a pre-defined threshold value is exerted on the head of an ATD for a time period of 3 ms or greater [32]. This criterion can also be applied to the chest to assess thoracic injury [33]. Another potential shortfall of the criteria used for pedestrian impact in CEN/TR 17420 is that, for head impact, only the primary impact between the vehicle and pedestrian is considered. Previous research highlighted that, for various light rail vehicles in operation in Europe, the secondary impact between the pedestrian and the road caused greater HIC values and therefore greater injury risk [34].

5.3. Recommendations and Future Work

5.3.1. Vehicle Safety Verification

Whilst the existing CVLR vehicle derogates from CEN/TR 17420 recommendations, it is possible to verify that the vehicle is safe for operation. With the dimensions, capacity, and mass of the CVLR vehicle being similar to those of buses and coaches (Table 8), and with similar operating principles, it is possible to present a case that the CVLR vehicle may be best suited to standards or best practices for buses and coaches with regards to pedestrian safety. Use of a framework such as the Common Safety Method for Risk Assessment (CSM RA) could be considered to formally review the case for derogation against frameworks that are specific to light rail (such as CEN/TR 17420) [35].

Table 8. Properties and dimensions of the CVLR vehicle compared to conventional buses and light rail vehicles.

Characteristic	CVLR Demonstrator Vehicle	Tram (CAF Urbos 3, Edinburgh)	Bus (Alexander Dennis Enviro200 [11.8 m])
Length	11.00 m	42.90 m	11.80 m
Width	2.65 m	2.65 m	2.44 m
Height	3.18 m	3.40 m	2.86 m
Unloaded mass	11 Tonnes	56 Tonnes	14.4 Tonnes
Passenger capacity	56 (20 seated)	250 (78 seated)	46 (all seated)
Railform	Standard-gauge	Standard-gauge	N/A (road vehicle)

The front-end design of buses and coaches must conform to regulation EU 2019/1892, which defines a three-dimensional envelope that the front end of a category M₃ vehicle must fit within [36]. This envelope (Figure 20a) defines that, if a vehicle has a flat frontal profile, there must be a minimum vertical rake angle of 3° at all points between a height of 1000 mm and 2000 mm above the ground, with a tapered angle at the vehicle edge. The shell of the CVLR vehicle has been assessed with the envelope and fits within the structure comfortably (Figure 20b–d).

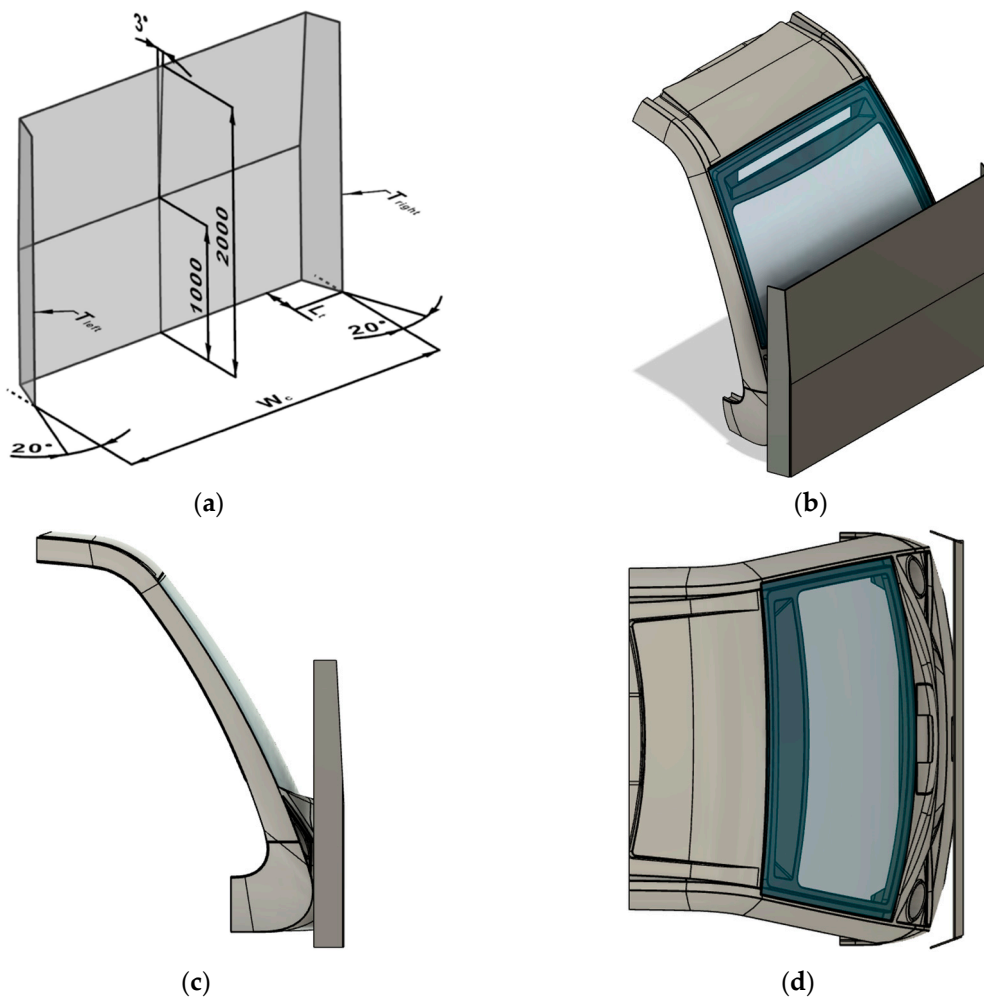


Figure 20. Images showing (a) the envelope for the vehicle frontal profile, category M₃ vehicles (EU 2019/1892), and the CVLR vehicle fitting within the envelope in (b) isometric view; (c) side-on view; and (d) top-down view.

Furthermore, Transport for London (TfL) has introduced the Bus Safety Standard (BSS), which is an additional more stringent set of recommendations for bus design going beyond the requirements of EU 2019/1892. From 2024, all new public transport vehicles purchased for operation within London by TfL must meet additional BSS criteria for frontal impact compatibility [37]. The BSS defines “optimised geometry” as a vehicle having geometry that “influences kinematics of a pedestrian during impact” [38]. Such features could include geometric features of the front-end design, such as curved profiles on the front end or a vertical rake angle along the front surface of the vehicle.

Whilst the front end of the CVLR vehicle does not meet the CEN/TR 17420 definition of optimised front-end design, the frontal curvature of the CVLR vehicle is more pronounced than that of a typical bus, with the CVLR vehicle also having a vertical rake angle of approximately 30° at head height. These factors would suggest that the CVLR vehicle could be defined as having optimised geometry by BSS recommendations. It could be validated that the geometry of the CVLR vehicle does influence pedestrian kinematics, given that low HIC₁₅ values were obtained in vehicle testing, even at 30 km/h. Mounting of the windscreen wipers is likely to be the only significant design change required to adhere to BSS, with mounting wipers at the top of the windscreen being required to meet impact protection criteria [39].

One of the challenges with the use of virtual modelling for conducting research in collision dynamics and biomechanics is the need to validate results with real-world testing scenarios. In order for a light rail vehicle, such as the CVLR vehicle, to be homologated to CEN/TR 17420, real-world dynamic testing would need to be conducted. Experiments completed in a virtual environment would need repetition with a real-world vehicle. The CEN/TR 17420 recommendations stipulate that, for validation of results of a vehicle, the deviation between results from virtual and real-world testing scenarios must not deviate by more than 20% [25]. This is specified by CEN/TR 17420 to account for differences between the real-world and virtual modelling of impact scenarios. Deviation between real-world and virtual scenarios may have many causes, including but not limited to the following: material cards for vehicle materials being unrepresentative of the physical components of a vehicle; contacts being incorrectly defined; and poorly defined meshing for vehicle components.

This report also only assesses one of the use cases and testing procedures for the CEN/TR 17420 framework for pedestrian crash compatibility of the CVLR vehicle. To comprehensively assess the CVLR vehicle to the CEN/TR 17420 technical report, pedestrian impact scenarios would need to be repeated with an HBM of a 6-year-old child. Following this, separate run-over scenarios, where the light rail vehicle starts the test conducting an emergency stop from 20 km/h, would need to be assessed for rescue mannequins representing both an adult male and a child.

To enable a more general understanding of the VRU safety of the CVLR vehicle, the number of scenarios modelled for vehicle-to-pedestrian interactions and collisions could be increased. Studies could be conducted to more thoroughly understand how injury risk to VRUs from the CVLR vehicle increases due to factors such as vehicle speed or the position of the VRU relative to the vehicle. Such research may identify particular areas of the vehicle where redesign or a facelift to the bodywork of the vehicle would reduce the injury risk to VRUs hit by the vehicle.

5.3.2. Transport Matrix Evolution

Considerations for the safety of VRUs on the road must account for the different types of VRU on urban road infrastructure and the ways in which the transportation matrix is set to change. Light rail systems, such as CVLR, are often developed within urban areas to provide attractive alternatives to cars for low-emission transportation. Other solutions, which are becoming more commonplace in urban environments in support of decarbonisation efforts, include micromobility solutions.

Micromobility is broadly defined by the Federal Highway Administration as a “small, low-speed transportation device” which can either be human or electric powered [39]. This definition includes bicycles and scooters, including bicycles and scooters with electric power systems. The micromobility sector is rapidly changing how people use transportation, with an estimated 16% of transportation completed by forms of micromobility in 2022, and this is expected to increase to 19% in 2035 [40]. Heinke’s forecast, published by McKinsey, states that micromobility solutions already make up more of the transportation matrix than walking, and this is set to increase over time. This highlights that the pragmatic approach to ensuring light rail vehicles are safe for all road users would be to consider the use cases of micromobility riders in VRU crash compatibility investigations.

To achieve this, use case scenarios for micromobility riders on or around light rail and road infrastructure should ideally be considered in VRU safety experiments for urban transportation means. Scenarios that define crash events for micromobility users such as riders of bicycles and e-scooters must be developed, with clear metrics for identifying injury risks outlined. This would enable a suitable VRU impact compatibility framework to be produced, which existing and new light rail vehicles could be assessed with.

Accounting for the safety of all VRUs and including micromobility users—as opposed to focusing solely on pedestrians as is the case in the CEN/TR 17420 safety assessment framework—would enable a more comprehensive understanding of vehicle safety to be achieved. This improved understanding of VRU safety would enable light rail vehicles to be safer for all road users and generate useful information about the risk levels for all road users. Assessment of the injury risks to micromobility riders using shared environments in particular ways, such as riding vehicles on the road as opposed to on the pavement, could also inform the future design of highway infrastructure.

6. Conclusions

As part of the Coventry Very Light Rail (CVLR) programme, a novel, battery-powered light rail vehicle has been developed, which operates on conventional steel wheels and standard-gauge rail tracks. The CVLR vehicle is road-going, similar to buses, enabling open traffic flow but is shorter than conventional buses or light rail vehicles (11 metres) to reduce vehicle mass. The CVLR vehicle is designed for “hop-on, hop-off” transport in urban areas such as Coventry, and would therefore frequently interact with Vulnerable Road Users (VRUs) such as pedestrians.

The technical report CEN/TR 17420 outlines a recommended framework for assessing the safety of pedestrians in collisions with light rail vehicles. Test conditions are prescribed for two tram-to-pedestrian scenarios in CEN/TR 17420: standing impact and lying-down run-over test scenarios. CEN/TR 17420 allows an exemption from tests for vehicles with specific geometric features of the front end, defined as an optimised front-end design.

In this article, the CVLR vehicle was assessed with the CEN/TR 17420 framework for the pedestrian impact scenario, at the prescribed impact speed of 20 km/h. An ATD of a 50th-percentile male was used, positioned standing at 15% and 50% distances between the centreline and the outer edge of the vehicle (15% TW and 50% TW, respectively). The vehicle met HIC_{15} requirements with a maximum value of 15.9 obtained, against the threshold of 1000 permitted in CEN/TR 17420. However, only a lateral deflection of 53.9 mm at a time of 15 ms after the end of contact between the vehicle and ATD was achieved, against the recommended 800 mm. This was due to the low impact speed and a lack of curvature of the front end.

Following recommendations by Lackner about typical tram-to-pedestrian collision speeds in a city environment of 30 km/h, the tests on the CVLR vehicle were repeated at the higher impact speed of 30 km/h. The HIC_{15} results increased approximately 8-fold to a maximum value of 120.9. The lateral displacement increased to 111.4 mm, still significantly below the specified 800 mm pass threshold of CEN/TR 17420.

A model was developed for the front end of the CVLR vehicle that would meet the CEN/TR 17420 definition of optimised front-end design (i.e., it would be exempt from

CEN/TR 17420 pedestrian impact testing). Pedestrian impact testing was performed at a 20 km/h impact speed, in line with CEN/TR 17420 specified test conditions. A maximum HIC₁₅ value of 63.7 was achieved, which, whilst higher than the CVLR vehicle results at 20 km/h, was still within the 1000 threshold. However, a lateral displacement of 592.7 mm was achieved within the prescribed time period, against the minimum 800 mm required.

It is highlighted that, whilst the optimised front-end geometry prescribed by CEN/TR 17420 does not meet testing requirements for lateral displacement of the ATD, the technical report would likely drive the adoption of optimised front-end geometry of light rail vehicles were CEN/TR 17420 codified as a legislated standard. It is also highlighted that a design that would meet lateral deflection requirements for CEN/TR 17420 would most likely lead to significant secondary impact with the road.

The CVLR vehicle was assessed against relevant bus standards (EU 2019/1892 and BSS) and was found to be mostly compliant with general requirements. To meet BSS requirements, it is noted that repositioning of the windscreen wipers from the base to the top of the windscreen wipers would be required.

Based on the findings of this article, the following recommendations are made:

1. Consideration should be made for the implications of an exempted front-end design in light rail standards for VRU impact events;
2. Impact speeds for tests should be increased to 30 km/h to be more representative of real-world, city-based events, and could result in an approximately 8-fold increase in HIC₁₅ values;
3. The HIC₁₅ requirement in CEN/TR 17420 may not capture the full consequences of a pedestrian impact event, and other metrics could be considered (e.g., “3 ms acceleration”);
4. VRU categories should be expanded to include other road users, such as cyclists and scooter users;
5. Standardised approaches to VRU safety, in a rapidly changing transport matrix, should be considered. This includes representing all types of VRUs, such as cyclists and scooter riders, when modelling VRUs in collision scenarios.

Supplementary Materials: The following supporting information can be downloaded at: <https://www.mdpi.com/article/10.3390/futuretransp4040057/s1>, Table S1: Material card used in LS-DYNA, automotive glass; Table S2: Material card used in LS-DYNA, carbon-fibre-reinforced polymer; Video S1: Video showing all collisions assessed in this paper.

Author Contributions: Conceptualisation, J.W. and D.J.H.; Data curation, C.J.D.B.; Formal analysis, C.J.D.B.; Funding acquisition, D.J.H.; Investigation, C.J.D.B.; Methodology, C.J.D.B. and S.S.; Project administration, S.S. and D.J.H.; Resources, D.J.H.; Software, C.J.D.B. and S.S.; Supervision, S.S. and D.J.H.; Validation, S.S., J.W. and D.J.H.; Visualisation, C.J.D.B.; Writing—original draft, C.J.D.B.; Writing—review and editing, S.S., J.W. and D.J.H. All authors have read and agreed to the published version of the manuscript.

Funding: The Coventry Very Light Rail project has been funded through the City Region Sustainable Transport Settlement by the West Midlands Combined Authority (WMCA).

Institutional Review Board Statement: Not applicable.

Informed Consent Statement: Not applicable.

Data Availability Statement: The data presented in this study are available on request from the corresponding author due to legal agreements.

Acknowledgments: The authors acknowledge the support of Coventry City Council in producing this work. The lead author acknowledges the Talent Development team at WMG, who have provided support throughout the course of this project.

Conflicts of Interest: Author James Winnett was employed by the company Penmark Limited. The remaining authors declare that the research was conducted in the absence of any commercial or financial relationships that could be construed as a potential conflict of interest.

References

1. Department for Transport. *Transport and Environment Statistics: 2023*; Department for Transport: London, UK, 2023.
2. Department for Business Energy and Industrial Strategy. *The Ten Point Plan for a Green Industrial Revolution*; Department for Business Energy and Industrial Strategy: London, UK, 2020.
3. UK Tram. *A Light Rail Strategy for the UK*; UK Tram: Birmingham, UK, 2022.
4. Department for Transport. *Light Rail and Tram Statistics (LRT)*; Department for Transport: London, UK, 2023.
5. Coventry City Council. *Coventry Very Light Rail Vehicle*; Coventry City Council: Coventry, UK, n.d. Available online: <https://www.coventry.gov.uk/coventry-light-rail/coventry-light-rail-vehicle> (accessed on 4 January 2024).
6. European Commission. *ITS & Vulnerable Road Users*; European Commission: Brussels, Belgium, n.d. Available online: https://transport.ec.europa.eu/transport-themes/intelligent-transport-systems/road/action-plan-and-directive/implementation-its-action-plan/its-vulnerable-road-users_en (accessed on 24 May 2024).
7. Transport Design International. *Coventry VLR-Project*; Transport Design International: Stratford-upon-Avon, UK, n.d. Available online: <https://transportdesigninternational.com/portfolio/coventry-vlr/> (accessed on 4 January 2024).
8. Department for Transport. *Road Traffic Estimates: Great Britain 2021*; Department for Transport: London, UK, 2022.
9. Department for Transport. *Reported Road Casualties Great Britain: Pedestrian Factsheet 2021*; Department for Transport: London, UK, 2022.
10. Dopravní Podnik Hlavního Města Prahy. *DPP Data Summary*; Dopravní Podnik Hlavního Města Prahy: Praha, Czech Republic, 2024. Available online: <https://www.dpp.cz/en/company/about-the-company/dpp-data> (accessed on 19 September 2024).
11. Lopot, F.; Tomsovsky, L.; Marsik, F.; Masek, J.; Kubovy, P.; Jezdik, R.; Sorfova, M.; Hajkova, B.; Hylmarova, D.; Havlicek, M.; et al. Pedestrian Safety in Frontal Tram Collision, Part 1: Historical Overview and Experimental-Data-Based Biomechanical Study of Head Clashing in Frontal and Side Impacts. *Sensors* **2023**, *23*, 8819. [CrossRef] [PubMed]
12. Gaca, S.; Franek, L. Pedestrian Fatality Risk as a Function of Tram Impact Speed. *Open Eng.* **2021**, *11*, 1105–1113. [CrossRef]
13. Federal Transit Administration. *Rail Safety Statistics Report: Rail Transit Safety Data 2007–2013*; Federal Transit Administration: Washington, DC, USA, 2016.
14. Martin, P.; Guy, I.; Carroll, J.; Radcliffe, J.; Hunt, R.; Dodd, M.; Knight, I.; Edwards, A.; McCarthy, M. *Published Project Report PPR977: The Transport for London Bus Safety Standard: Vulnerable Road User (VRU) Frontal Crashworthiness: Evaluation of Safety Measure*; Transport Research Laboratory: Wokingham, UK, 2020.
15. Edwards, A.; Barrow, A.; O'Connell, S.; Krishnamurthy, V.; Khatry, R.; Hylands, N.; McCarthy, M.; Helman, S.; Knight, I. *Published Project Report PPR819: Analysis of Bus Collisions and Identification of Countermeasures*; Transport Research Laboratory: Wokingham, UK, 2018.
16. Martin, P.; Radcliffe, J.; Qasim, M.; Guy, I. Enhanced Bus Front End Geometries for Improved Pedestrian Crashworthiness. In Proceedings of the International Research Council on the Biomechanics of Injury Conference, Online, 8–10 September 2020.
17. Schmitt, K.-U.; Niederer, P.F.; Muser, M.H.; Walz, F. *Trauma Biomechanics*, 3rd ed.; Springer: Berlin/Heidelberg, Germany, 2010. [CrossRef]
18. Mariotti, G.V. Head Injury Criterion: Mini Review. *Am. J. Biomed. Sci. Res.* **2019**, *5*, 406–407. [CrossRef]
19. Henn, H.-W. Crash Tests and the Head Injury Criterion. *Teach. Math. Its Appl.* **1998**, *17*, 162–170. [CrossRef]
20. European New Car Assessment Programme. *Assessment Protocol—Adult Occupant Protection*; Euro NCAP: Leuven, Belgium, 2023.
21. Hertz, E. A Note on the Head Injury Criterion (HIC) as a Predictor of the Risk of Skull Fracture. In Proceedings of the 37th Annual Conference of the Association for the Advancement of Automotive Medicine, San Antonio, TX, USA, 4–6 November 1993; Association for the Advancement of Automotive Medicine (AAAM): Des Plaines, IL, USA, 1993; pp. 73–80.
22. Kleinberger, M.; Sun, E.; Eppinger, R.; Kuppa, S.; Saul, R. Development of Improved Injury Criteria for the Assessment of Advanced Automotive Restraint Systems. *NHTSA Docket* **1998**, *4405*, 12–17.
23. Eppinger, R.; Sun, E.; Bandak, F.; Haffner, M.; Khaewpong, N.; Maltese, M.; Kuppa, S.; Nguyen, T.; Takhounts, E.; Tannous, R.; et al. *Development of Improved Injury Criteria for the Assessment of Advanced Automotive Restraint Systems—II*; National Highway Traffic Safety Administration: Washington, DC, USA, 1999.
24. Office for Rail and Road. *Light Rail and Tramways*; Office of Rail and Road: London, UK, n.d. Available online: <https://www.orr.gov.uk/about/who-we-work-with/railway-networks/light-rail-tramways> (accessed on 7 October 2024).
25. Comité Européen de Normalisation. *Railway Applications—Vehicle End Design for Trams and Light Rail Vehicles with Respect to Pedestrian Safety*; European Committee for Standardization: Brussels, Belgium, 2020.
26. Lackner, C.; Heinzl, P.; Rizzi, M.C.; Leo, C.; Schachner, M.; Pokorny, P.; Klager, P.; Buetzer, D.; Elvik, R.; Linder, A.; et al. Tram to Pedestrian Collisions—Priorities and Potentials. *Front. Future Transp.* **2022**, *3*, 913887. [CrossRef]
27. Lackner, C. Parameter Study on Pedestrian Impacts onto a Light Rail Vehicle. Bachelor's Thesis, Technische Universität Wien, Vienna, Austria, 2020.
28. Livermore Software Technology Corporation. *HYBRID III ADULT FAST*. Ansys LS-DYNA. Available online: <https://lsdyna.ansys.com/dummies/> (accessed on 5 April 2024).
29. Liu, Y.; Carnegie, C.; Ascroft, H.; Li, W.; Han, X.; Guo, H.; Hughes, D.J. Investigation of Adhesive Joining Strategies for the Application of a Multi-Material Light Rail Vehicle. *Materials* **2021**, *14*, 6991. [CrossRef] [PubMed]
30. Osnes, K.; Kreissl, S.; D'Haen, J.; Børvik, T. Modelling of Fracture Initiation and Post-Fracture Behaviour of Head Impact on Car Windshields. In Proceedings of the 13th European LS-DYNA Conference, Ulm, Germany, 5–7 October 2021.

31. Transport for London. *Road Danger Reduction Dashboard*; Transport for London (TfL): London, UK, n.d. Available online: <https://tfl.gov.uk/corporate/publications-and-reports/road-safety#on-this-page-1> (accessed on 2 February 2024).
32. Boggess, B.M.; Foreman, G.G. Mass-Based Considerations for Head Injury Protection Development. In Proceedings of the 20th International Technical Conference on the Enhanced Safety of Vehicles (ESV), Lyon, France, 18–21 June 2007.
33. Carollo, F.; Virzi Mariotti, G.; Scalici, E. Biomechanics Parameters in the Vehicle-Cyclist Crash with Accident Analysis in Palermo. In Proceedings of the NAUN Conference ECME'14, Florence, Italy, 22–24 November 2014; Recent Advances in mechanical Engineering, pp. 139–148.
34. Weber, T.; Muser, M.; Schmitt, K.-U. Optimising the Design of Tramways to Mitigate Injury Risk in Pedestrian Impacts. In Proceedings of the IRCOBI Conference 2015, Lyon, France, 9–11 September 2015; International Research Council on the Biomechanics of Injury: Lyon, France, 2015; pp. 339–349.
35. Office of Road and Rail. *Common Safety Method for Risk Evaluation and Assessment*; Office of Road and Rail: London, UK, 2018.
36. European Commission. *Amending Regulation (EU) No 1230/2012 as Regards Type-Approval Requirements for Certain Motor Vehicles Fitted with Elongated Cabs and for Aerodynamic Devices and Equipment for Motor Vehicles and Their Trailers*; European Commission/European Union: Brussels, Belgium, 2019.
37. Transport for London. *Bus Safety Roadmap for New Build Buses*; Department for Transport: London, UK, n.d. Available online: <https://content.tfl.gov.uk/bus-safety-road-map-for-new-build-buses.pdf> (accessed on 7 October 2024).
38. Transport Research Laboratory. *Bus Safety Standard: Future Roadmap*; Transport Research Laboratory: London, UK, 2020.
39. Price, J.; Blackshear, D.; Blount, W., Jr.; Sandt, L. *Micromobility: A Travel Mode Innovation*; Public Roads Magazine: Washington, DC, USA, 2021.
40. Heineke, K.; Laverty, N.; Möller, T.; Ziegler, F. *The Future of Mobility*; McKinsey & Company: New York, NY, USA, 2023.

Disclaimer/Publisher's Note: The statements, opinions and data contained in all publications are solely those of the individual author(s) and contributor(s) and not of MDPI and/or the editor(s). MDPI and/or the editor(s) disclaim responsibility for any injury to people or property resulting from any ideas, methods, instructions or products referred to in the content.